The International Journal of Advanced Manufacturing Technology (2020) 108:1701–1712
https://doi.org/10.1007/s00170-020-05530-4

ORIGINAL ARTICLE

Study on the influence of micro-textures on wear mechanism of cemented carbide tools

Junsheng Zhang [1] · Haidong Yang [1] · Shunhua Chen [1] · Huohong Tang [1]

Received: 14 February 2020 / Accepted: 20 May 2020 / Published online: 30 May 2020

Abstract
Wear behavior of micro-textured insert with lubrication was studied. Micro-pits with different diameters (80–200 μm), depths (3–10 μm), and area occupancies (10–30%) were manufactured on the tool rake face near the main cutting edge. Experimental research was conducted to reveal the effect of micro-pits on tool-chip interface friction characteristics. Besides, the texture parameter with better tribological characteristics was selected to study the wear mechanism of textured insert. Scanning electron microscopy analysis was conducted on the worn area of rake face. The results confirmed that the micro-textures can effectively reduce the average shear strength of rake face and actual tool-chip contact length during machining. The best average friction coefficient can be obtained with texture diameter of 170 μm, depth of 7 μm, and area occupancy of 20%. Adhesive wear, diffusion wear, and oxidation wear appeared on the worn area of rake face. The micro-textures can effectively reduce the diffusion wear and suppress the built-up edge (BUE) by improving tool-chip interface friction characteristics. The findings are of significance for enhancing the application of textured insert with excellent tribological characteristics.

Keywords Micro-texture · Wear behavior · Average friction coefficient · Cutting force · Adhesive wear

1 Introduction

Wear behavior between the tool-chip interface has always been an important issue which can affect the cutting performance. Recently, micro-texture technology has made considerable process in the field of tribology. Wear behavior between the friction pairs can be effectively improved with micro-texture and lubrication. It also shows great prospects in the application of metal-cutting process. The introduction of micro-texture on the certain place can improve the friction characteristics at the tool-chip interface with lubrication. Therefore, micro-textured cutting tools have drawn a great deal of research attention [1, 2]. Arslan et al. [3] presented a review article and pointed out that the cutting performance, wear behavior, and friction characteristics can be improved with micro-textured inserts.

In terms of cutting performance, many studies were conducted with micro-textured inserts [4, 5]. The effect of micro-textures on lubrication behavior with cemented carbide tools was studied by Ge et al. [6]. It showed that the lubricants can enter the tool-chip interface through micro-grooves, and main cutting force can be reduced by more than 20%. The micro-textured insert can also be used to improve the cutting performance during the machining of titanium. Liu et al. [7] pointed out that the introduction of micro-textures on WC-10Ni_3Al cutting tools can effectively improve the cutting performance and wear behavior on the insert worn area during the turning of Ti6Al4V. Duan et al. [8, 9] pointed out the derivative cutting behavior with micro-textured tools, which would accelerate texture wear and lead to a severer tool-chip interface friction. The micro-textures can also be manufactured on a sapphire cutting tool, where the friction coefficient decreased about 8% on average, and the adhesion length was reduced by 28% [10]. Besides, built-up edge stabilization and tool wear of micro textured cemented carbide tools were also investigated. It confirmed that the micro-textures can improve the wear behavior when compared with untextured tools in terms of corner radius wear [11]. The micro-textured tools can also be used to improve the wood cutting performance [12]. The investigations presented above confirm that the introduction of micro-texture on the certain place of insert can indeed improve the cutting performance.

✉ Haidong Yang
yanghaidonghfut@126.com

1 Hefei University of Technology, Hefei 230009, China

Furthermore, many studies were conducted on the optimization of texture parameters and forms. Liu et al. [13] presented that the process of lubricant entering the tool-chip interface was effectively influenced by the texture parameters. The size, shape, and combination of micro-textures should be optimized with taking both lubrication and strength of insert rake face into consideration. Ye et al. [14] optimized the texture parameters and confirmed that the micro-grooves with groove spacing of 100 μm, groove depth of 20 μm, and groove width of 50 μm can improve the cutting performance and wear behavior more significantly. Sun et al. [15] presented the cutting performance of hybrid-textured tools and analyzed the process of cutting fluids entering the tool-chip interface through hybrid textures. Micro-textures can also be used for machining heat-resistant superalloys (HRSA) [16]. Cylindrical dimples on the rake face and square pyramids on the flank face were manufactured on the carbide tools which were used for machining alloy 718. The research confirmed that the micro-textures on the rake and flank face can effectively improve the wear behavior, leading to an increase of tool life about 30%. In order to optimize the texture parameters, orthogonal cutting of aluminum was conducted with different texture diameters (50, 100, and 150 μm), depths (10, 25, and 50 μm), and pitches (50, 100 and 150 μm) [17]. Pang et al. [18, 19] designed conical micro-grooved texture and studied the effect of the new texture form on tool-chip interface friction coefficient with lubrication. It confirmed that the conical micro-grooved texture can also improve the friction characteristics and reduce the friction coefficient. Additionally, statistical methods have shown the potential to optimize the texture parameters [20].

In recent years, self-lubricating and dry manufacturing were proposed for their environment friendly properties. Gajrani et al. [21] discussed the cutting performance of textured tools without cutting fluids. Afterwards, textured tools coated with MoS_2 solid lubricant presented 23.5% lower tool-chip interface temperature and 41.06% reduction in the cutting force when compared with untextured tools [22]. Xing et al. [23] designed nano-textured inserts with WS_2/Zr coating and showed better friction characteristics during dry cutting. A comparative study of self-lubricating inserts was conducted by Sharma and Pandey [24], and it showed that the cutting forces and chip thickness ration can be reduced for more than 30% and 3%, respectively, with hybrid textured inserts. Feng et al. [25] applied the micro-texture to ceramic insert and confirmed that the cutting performance and wear behavior can also be improved without lubrication. Kang et al. [26] presented experimental studies on micro-textured inserts to improve the tool-chip interface friction characteristics. The cutting performance was studied in terms of cutting force, chip form, and wear behavior. It also pointed out that the advantages would be weakened when the micro-textures disappeared during the dry machining.

However, the studies about textured insert mainly focused on the cutting performance [27, 28], new micro-texture form [18, 19], and self-lubricating [21], as well as the lubrication mechanisms of micro-textures. The detailed investigations on the wear mechanism of micro-textured inserts have rarely been reported. Appropriate micro-textures can effectively improve the cutting performance and tool wear. However, micro-textures can also destroy the strength of the insert and reduce the tool life, if they are not properly used. A further investigation in the wear mechanism of micro-textured inserts can present the advantages of micro-textures in tool wear and improve the tool life. Therefore, in this work, the wear mechanism of micro-textured inserts was presented by both experimental observations and theoretical analysis. The wear mechanism in terms of adhesion, diffusion, and oxidation was analyzed in detail during the machining of AISI 1045 steel with micro-textured cemented carbide tools. The texture parameters were optimized with experiments to research the wear mechanism of textured inserts. In order to show the wear behavior more clearly, scanning electron microscopy (SEM) and energy dispersive spectrometer (EDS) were conducted on the worn area of rake face. This research may have an important contribution to revealing the wear mechanism of micro-textured inserts.

2 Experimental details

2.1 Workpiece and tool material

The workpiece used in this research is AISI 1045 steel bar. Table 1 presents the compositions and physical performance of AISI 1045 steel [18]. The workpiece used in this research is a metal bar with diameter of ϕ90 mm and length of 400 mm. The WC-TiC/Co cemented carbide insert (YT15 uncoated) used in this research is commercially available, and the compositions and physical performance of YT15 inserts are shown in Table 2.

2.2 Cutting conditions

The research on the wear mechanism of micro-textured cemented carbide tools was carried out on a CA6140 lathe, which was equipped with a three-dimensional dynamometer. The working geometrical parameters of the cemented carbide tools are shown in Table 2. The water-miscible cutting fluid (JR3A, 2.5%) was prepared. During machining, the insert rake face was supplied with continuous cutting fluids, and the flow rate was set to 10 L/min. The cutting force was measured with a three-dimensional dynamometer Kistler 9257B. The dynamometer has high resolution and reliability. The measuring ranges of F_x, F_y, and F_z are 5 kN, 5 kN, and 10 kN,

Table 1 Compositions and physical performance of AISI 1045 steel

Compositions (wt%)							
C	Si	Mn	Cr	Ni	Cu	P	S
0.42–0.5	0.17–0.37	0.5–0.8	≤ 0.25	≤ 0.25	≤ 0.25	≤ 0.035	≤ 0.035
Physical performance							
Density (g/cm^3)	Hardness (HRC)		Tensile strength (MPa)		Yield strength (MPa)		
7.85	30		600		355		

respectively. The sensitivity of F_x (F_y) is − 7.5 *pC*/*N* and − 3.7 *pC*/*N* for F_z.

2.3 Tool texturing

The micro-textures on insert rake face were manufactured with a fiber laser engraving machine YLP-F10. It has a wavelength of 1.06 μm, out power of 0–10 W, and plus frequency of 20 to 100 kHz. Before the texturing process, the YT15 insert especially for the rake face was cleaned with acetone. During laser texturing process, many burrs may come up near the edges of the textures. Then, the rake face of the textured insert was polished with abrasive paper to eliminate these burrs. Finally, ultrasonic cleaning was conducted to remove the residual pollutants in the textures. Figure 1 presented the diagram of micro-textures processing.

The micro-textures selected in this research were micro-pits for their symmetrical pattern, which would yield more consistent results [17]. Previous studies confirmed that micro-pit textures had better wear resistance performance, as compared with micro-groove textures [11]. Micro-pits can exhibit better performance than micro-grooves especially under a severe lubricating condition [29]. The texture parameters (diameter, depth and area occupancy) can also affect the wear resistance performance during the machining with lubrication. Therefore, based on these researches mentioned above and the limit of fiber laser engraving machine, the texture parameters and machine parameters during the texture manufacture process were presented in Table 3. Here, texturing times were the number of repetitional processing times used to change the depth of micro-pit. Area occupancy was presented in Fig. 2. The texture parameters were checked with Talysurf CCI Lite non-contact 3D optical profilometer. Micromorphology of the textures on the rake face was shown in Fig. 3. To reveal the influence of texture diameter on cutting performance, the depth and area occupancy will keep constant when diameter ranges from 80 to 200 μm. Same method was conducted for the study of texture depth and area occupancy. It should be noticed that T4, T8, and T14 have the same texture parameters. The purpose of this design is to make the relationship between each parameter and cutting performance clearer.

Table 2 Compositions, physical performance, and working geometrical parameters of YT15 inserts

<table>
<tr><th colspan="3">Compositions (wt%)</th><th colspan="3">Physical performance</th></tr>
<tr><td>WC</td><td>TiC</td><td>Co</td><td>Density (g/cm^3)</td><td>Hardness (HRA)</td><td>Flexural strength (MPa)</td></tr>
<tr><td>79</td><td>15</td><td>6</td><td>11.5</td><td>91</td><td>1150</td></tr>
<tr><td colspan="6">Working geometrical parameters</td></tr>
<tr><td colspan="3" rowspan="5">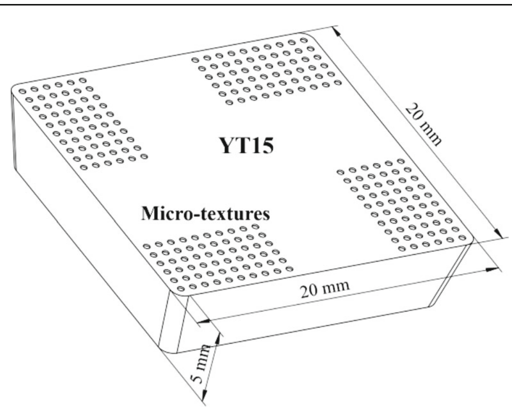
</td><td colspan="2">Rake angle r_{oe}</td><td>-8°</td></tr>
<tr><td colspan="2">Clearance angle α_{oe}</td><td>18°</td></tr>
<tr><td colspan="2">Inclination angle λ_{se}</td><td>0°</td></tr>
<tr><td colspan="2">Side cutting edge angle K_{re}</td><td>42°</td></tr>
<tr><td colspan="2">Corner radius r_{ε}</td><td>0.8 *mm*</td></tr>
</table>

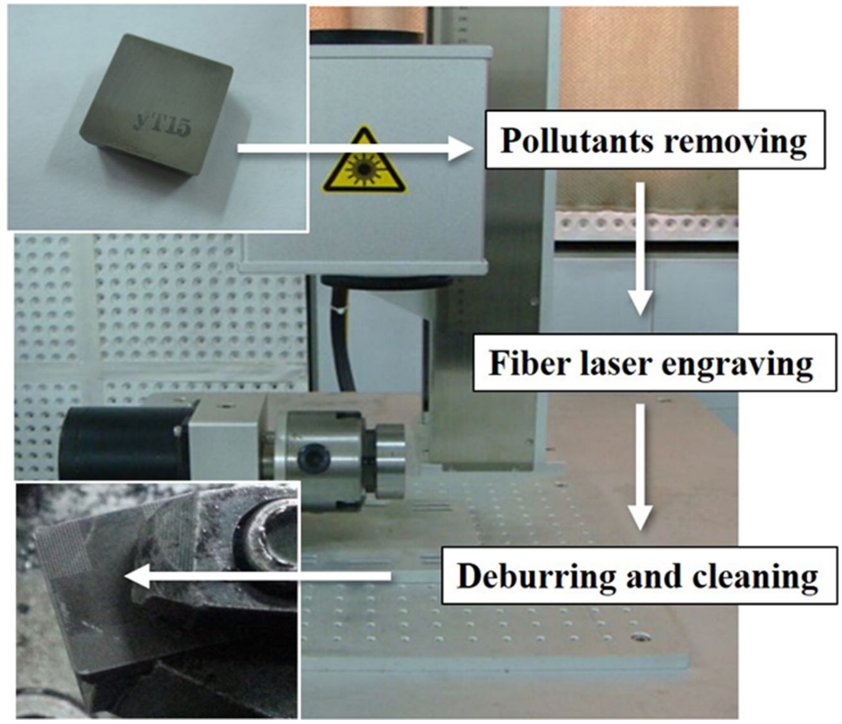

Fig. 1 Diagram of micro-textures processing

2.4 Cutting tests and measurements

The experiment was conducted with the CA6140 lathe and lubrication. The textured inserts were named T1–T15 with different texture parameters, as shown in Table 3. The untextured inserts were named T0 for comparison. The hardness of 1045 steel was relatively small. In order to obtain a better surface roughness, a higher cutting speed, lower depth of cut, and feed rate were selected during machining. In this part, the cutting parameters were cutting speed $v = 120$ m/min, depth of cut $a_p = 0.5$ mm, and feed rate $f = 0.1$ mm/r. The cutting tests were conducted at room temperature (24 °C). Cutting force was measured with the three-dimensional dynamometer during machining. The cutting tests were performed

Table 3 Texture parameters and laser processing parameters used in this research

	Texture parameters			Laser processing parameters		
No.	Diameter *d* (*um*)	Depth *h* (*um*)	Area occupancy *w* (%)	Scanning Speed (mm/s)	Texturing times	Power (W)
T1	80					
T2	110					
T3	140	7	20	270	4	2.9
T4	170					
T5	200					
T6			10			
T7			15			
T8	170	7	20	270	4	2.9
T9			25			
T10			30			
T11		3			2	2.9
T12		4			2	3.1
T13	170	5	20	270	3	2.9
T14		7			4	2.9
T15		10			5	3.0

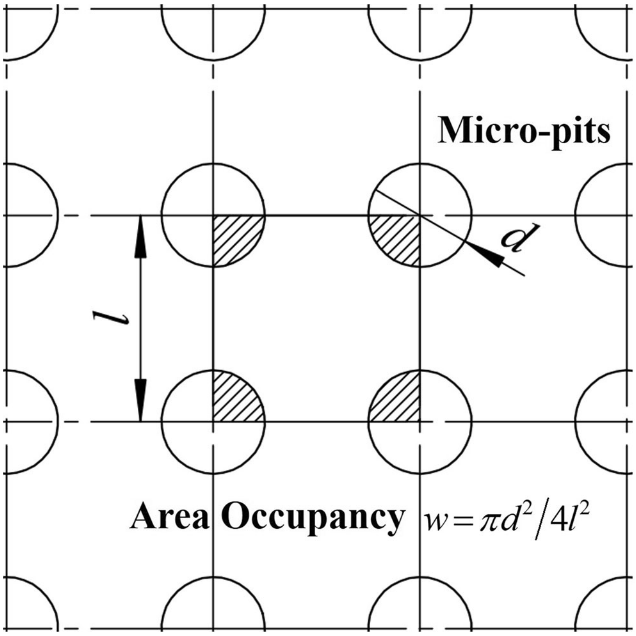

Fig. 2 Diagram of area occupancy

three times for each condition, and the average values were recorded and calculated. Figure 4 presents the experimental setup during the machining.

The friction characteristics of tool-chip interface can directly influence the wear behavior on rake face. The introduction of micro-textures can effectively improve the tool-chip interface friction characteristics. To make the advantages of micro-textures clearer and study the wear behavior of textured inserts, the texture parameters with lower tool-chip interface friction coefficient were selected. Based on the experimental results, T14 insert was selectedm and untextured insert (T0) was used for comparison. To study the wear behavior of textured inserts, continuous cutting was conducted during the tests. The machining time was set as 210 s for each sample, and the cutting parameters were enlarged (cutting speed $v=$

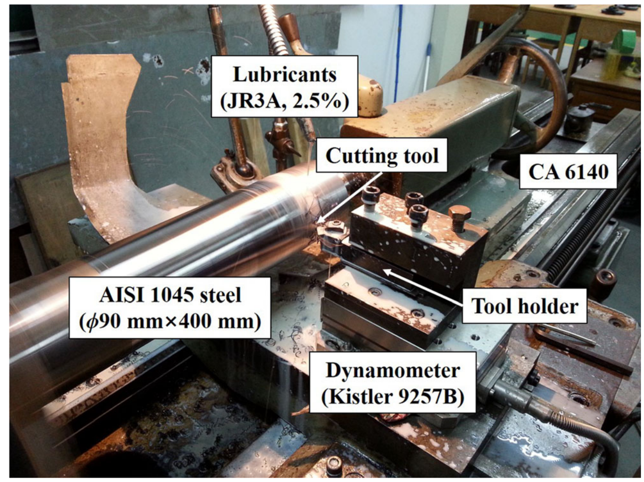

Fig. 4 The experimental setup during the machining

Fig. 3 Micromorphology of textures on the T14 insert rake face

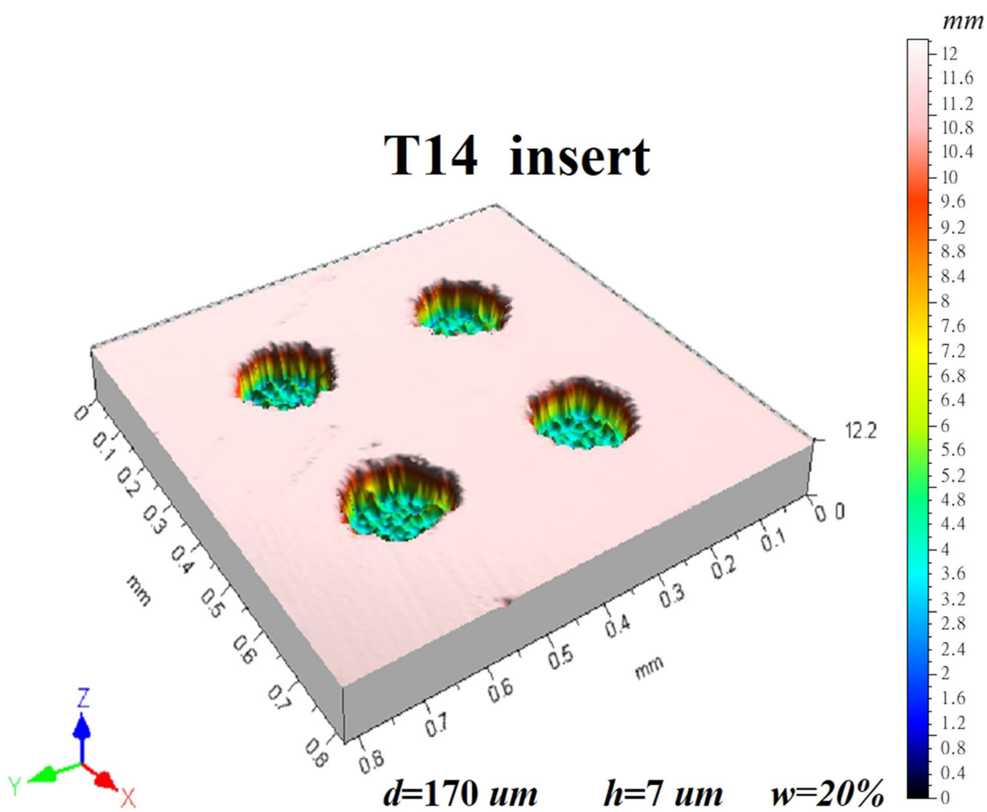

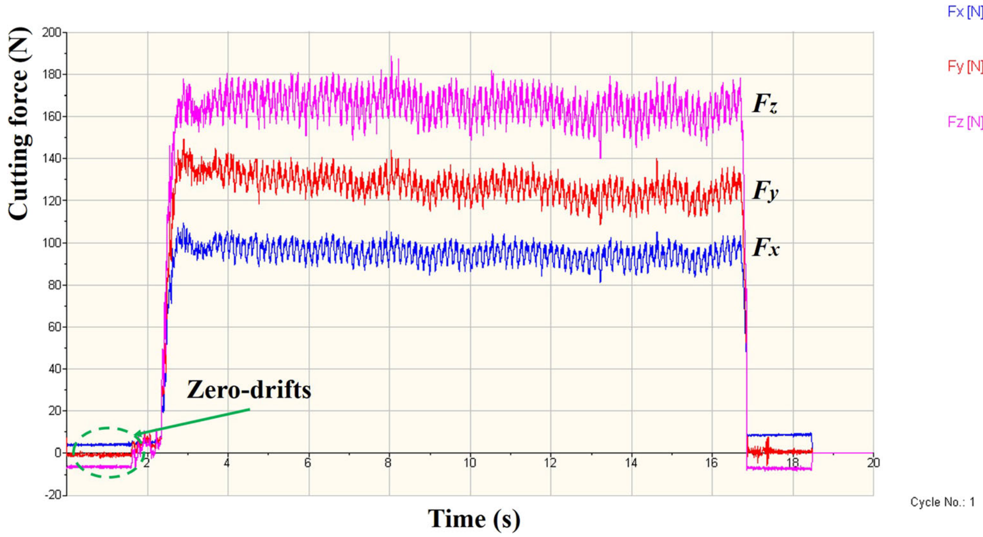

Fig. 5 Result of cutting forces with T14 inserts at the speed of 120 m/min

200 m/min, depth of cut $a_p = 0.5$ mm, and feed rate $f =$ 0.14 mm/r) to obtain obvious wear marks. The cutting forces were measured throughout the machining. To reveal the worn morphology and chemical composition on the rake face, SEM and EDS analysis were conducted on the worn area near the main cutting edge (T14 and T0).

3 Results and discussion

3.1 Analysis of cutting forces

Figure 5 presents the results of cutting forces obtained from the dynamometer with T14 insert with cutting speed of 120 m/min. During the recording of cutting forces, the zero drifts of the dynamometer were removed. The main cutting force F_z is larger than the radial force F_y and axial force F_x. The cutting forces of the textured inserts (T1–T15) and untextured insert (T0) at the speed of 120 m/min with lubrication are presented in Fig. 6. The result shows that the cutting forces of textured inserts are much lower than untextured insert. It also confirms that micro-pits on the rake face can effectively reduce the cutting forces by changing the tool-chip interface friction characteristics with lubrication.

Here, the machining process stays in the boundary lubrication condition. There is a lubrication layer between the tool rake face and chip. It cannot completely separate the

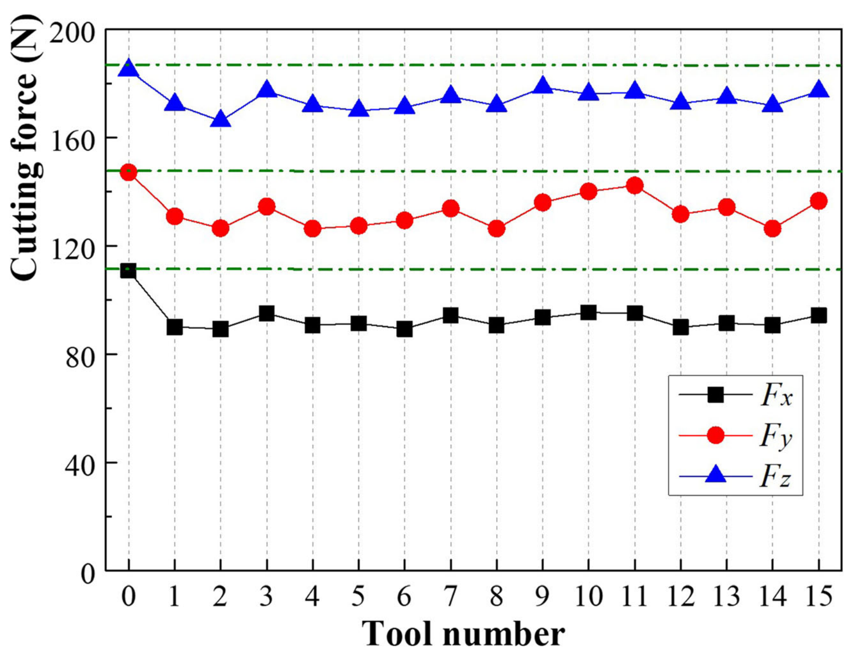

Fig. 6 Cutting forces of textured inserts (T1–T15) and untextured insert (T0) at the speed of 120 m/min with lubrication

workpiece and insert during the machining. Therefore, the frictional force of the tool-chip interface F_f can be express as:

$$F_f = A_r\tau_c = A_r\left[k\tau_b + (1\text{-}k)\tau_f\right] \quad (1)$$

where A_r is the total contact area of the tool-chip interface, τ_c is the average shear strength, k is the metal adhesion area percentage in the total contact area, τ_b is the shear strength of the metal adhesion area, and τ_f is the shear strength of the lubrication layer. According to Eq. (1), the frictional force is mainly depended on the percentage of metal adhesion area. Because the shear strength of workpiece material and lubrication layer is constant, the introduction of micro-textures can reduce the metal adhesion area, which will enlarge the contact area of lubricant. The shear strength of the lubrication layer is much lower than that of metal adhesion area. Finally, the average shear strength τ_c and frictional force F_f will decrease.

The frictional force can also be calculated by:

$$F_f = A_r\tau_c = a_w l_f \tau_c \quad (2)$$

where the resultant force F_r, the main cutting force F_z, and radial force F_y can be expressed as [25].

$$F_r = F_f/\sin\beta = a_w l_f \tau_c/\sin\beta \quad (3)$$

$$F_y = F_r\sin(\beta - \gamma_0) = a_w l_f \tau_c \sin(\beta - \gamma_0)/\sin\beta \quad (4)$$

$$F_z = F_r\cos(\beta - \gamma_0) = a_w l_f \tau_c \cos(\beta - \gamma_0)/\sin\beta. \quad (5)$$

Here, l_f is the actual tool-chip contact length, and a_w is the cutting width. Accordingly, it indicates that there is a linear relationship between the cutting forces (F_r, F_y, and F_z) and average shear strength τ_c and actual tool-chip contact length l_f. The introduction of micro-textures can reduce the average shear strength, as shown in Eq. (1). In addition, the introduction of micro-textures can also reduce the actual tool-chip contact length during the machining. Therefore, the resultant force F_r, main cutting force F_z, and radial force F_y will be improved, as shown in Fig. 6.

3.2 Friction characteristics

Friction characteristics of the insert worn area can directly influence the cutting performance and tool wear. In order to reveal the tool-chip interface friction characteristics, average friction coefficient was calculated based on the cutting force results. The average friction coefficient can be expressed with following formulas:

$$\tan\ (\beta - \gamma_0) = F_y/F_z \quad (6)$$

$$\beta = \tan^{-1}\ (F_y/F_z) + \gamma_0 \quad (7)$$

$$u = \tan\beta = \tan\left[\tan^{-1}\ (F_y/F_z) + \gamma_0\right] \quad (8)$$

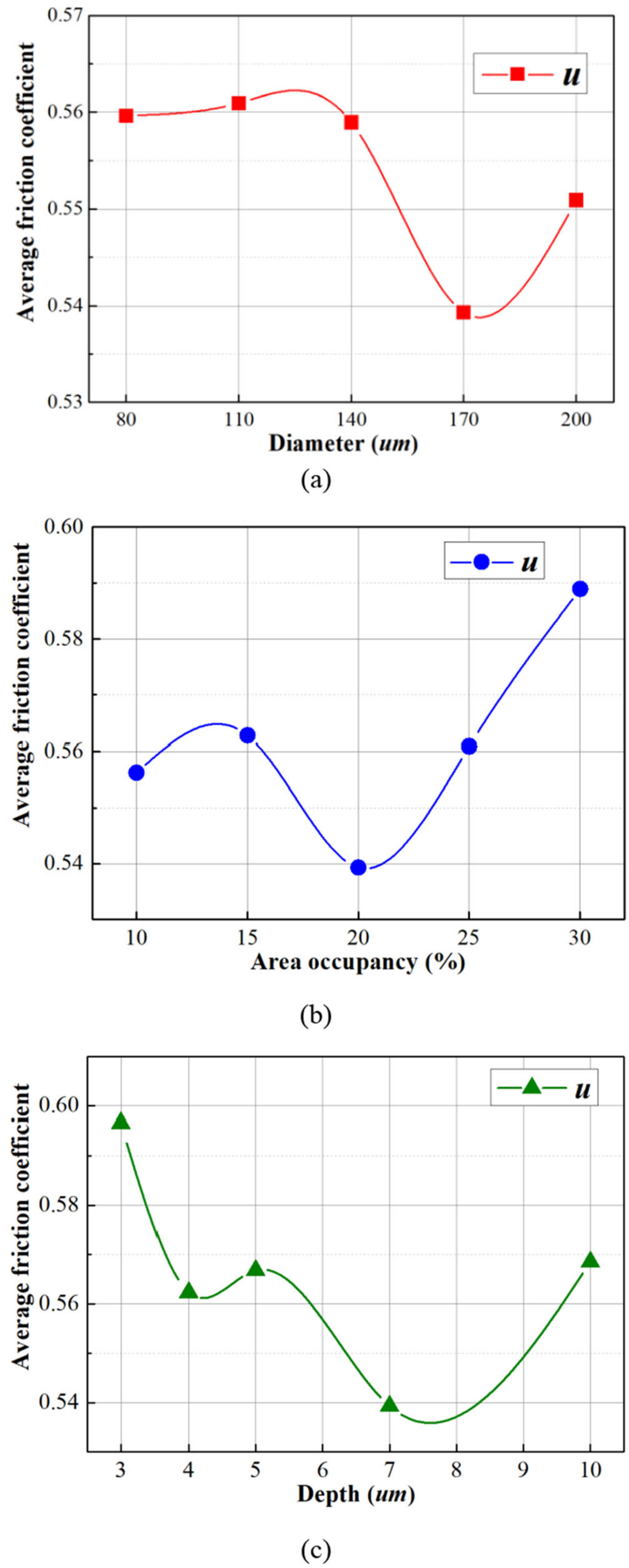

Fig. 7 Average friction coefficients of textured inserts **a** T1-T5, **b** T6-T10, and **c** T11-T15

where β is the friction angle, γ_0 is the rake angle, and u is the average friction coefficient. The tool-chip interface average friction coefficients of textured inserts at the speed of 120 m/min with lubrication are presented in Fig. 7. It reveals the relationship between texture parameters (diameter, depth, and area occupancy) and average friction coefficient directly. Here, the average friction coefficient of untextured insert T0 is 0.589. Compared with untextured insert, the average friction coefficients of textured inserts are effectively reduced. Figure 7a shows that the average friction coefficient decreases first and then increases with the diameter ranging from 80 to 200 μm. The average friction coefficient reaches the lowest value when the diameter is 170 μm. The same variation trend appears in Fig. 7b, c. The best texture parameters with diameter $d = 170$ μm, depth $h = 7$ μm, and area occupancy $w = 20\%$ are therefore obtained, at which the tool-chip interface has better wear behavior.

The average friction coefficient mainly depends on friction characteristics of insert worn area. The normal stress on the rake face near to the main cutting edge can be presumed to decrease gradually from the maximum value to zero. The actual tool-chip contact length l_f can be expressed with [30, 31].

$$l_f = a_w \frac{\xi + 2}{2} \cdot \frac{\sin(\phi + \beta - \gamma_0)}{\sin\phi \ \cos\beta} \tag{9}$$

where ξ is the stress distribution exponent constant, and ϕ is the shear angle. Combining Eqs. (3) and (9), the resultant force F_r can be expressed with:

$$F_r = a_w^2 \frac{\xi + 2}{2} \cdot \frac{\sin(\phi + \beta - \gamma_0)}{\sin\phi \ \cos\beta \ \sin\beta} \cdot \tau_c \tag{10}$$

Furthermore, the resultant force F_r can also be expressed with workpiece material shear strength τ_s, as follows [32]:

$$F_r = \frac{a_w a_c \tau_s}{\sin\phi \ \cos(\phi + \beta - \gamma_0)} \tag{11}$$

where τ_s is the workpiece material shear strength, and a_c is the cutting thickness. Then, the relationship between the friction angle β and the average shear strength τ_c is obtained as follows based on Eqs. (10) and (11):

$$\sin 2\beta = \frac{a_w \tau_c (\xi + 2) \sin 2(\phi + \beta - \gamma_0)}{2 a_c \tau_s} \tag{12}$$

Here, the friction angle is less than 45°, then the friction angle and average friction coefficient u increase linearly with average shear strength τ_c. Therefore, the average friction coefficient u can be improved with micro-textures, which is mainly due to the decreasing of average shear strength τ_c at the tool-chip interface.

On the other hand, the variation of average friction coefficient u can also be explained with shear angle ϕ, which can be calculated by [6].

$$\phi = \pi/4 + \gamma_0/2 - \beta/2 \tag{13}$$

It can directly reflect deformation and show the variation trend of friction angle. The introduction of micro-textures can also increase the shear angle as shown in previous researches [15], which will result in less friction angle and reduce average friction coefficient u.

The texture parameter is also important because the perfect combination of texture parameter can have a better lubrication condition and wear behavior. The increasing of texture diameter and area occupancy can directly reduce the metal adhesion area percentage, which will result in a lower average shear strength and average friction coefficient. However, the oversized texture diameter and area occupancy will destroy the strength of the insert, which will lead to a serious wear behavior and an increasing of average friction coefficient, as shown in Fig. 7a, b. These results indicate that the micro-pits with suitable parameters can have a better cutting performance

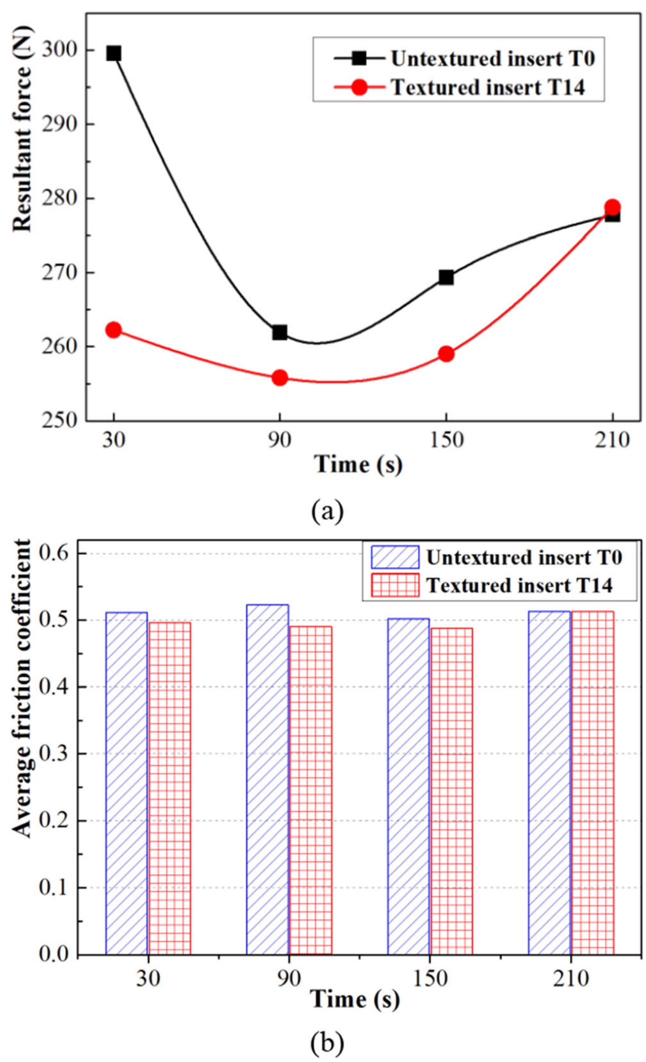

Fig. 8 Resultant force (**a**) and average friction coefficient (**b**) throughout the machining

by reducing the average shear strength τ_c of the tool-chip interface.

3.3 Wear behavior

Wear behavior at the tool-chip interface can influence the tool life. The introduction of micro-textures on the rake face can improve the wear characteristics at the tool-chip interface and cutting performance with lubrication. Continuous cutting was conducted in this part with T14 and T0 inserts under lubricating condition. Here, the cutting parameters were enlarged to obtain obvious wear marks. The resultant force F_r and average friction coefficient throughout the machining were shown in Fig. 8. The resultant force and average friction coefficient of textured insert were lower than those of untextured insert during the machining. This is mainly due to the micro-textures could reduce the average shear strength and improve the tool-chip interface wear behavior. Besides, roughness of machined surface was measured with the surface profilometer HT-SURF10000. The results were shown in Fig. 9, and it indicated that the machined surface roughness of T14 was almost the same as that of T0. To study the wear mechanism of textured insert, worn morphology and chemical composition on the worn area of T14 and T0 inserts were obtained with SEM and EDS analysis. Figures 10 and 11 presented the SEM and EDS results of T14 and T0 inserts, respectively.

Usually, the wear behavior on the rake face can be performed in terms of abrasive wear, adhesive wear, diffusion wear, and oxidation wear. Abrasive wear is mainly due to the hard grains from workpiece material and dislodged grains from insert. Here, the abrasive marks are not obvious in Figs. 10 and 11. The reason is that the hardness of the insert material is much higher than the workpiece material.

Adhesion on the rake face is observed both for the textured insert T14 and untextured insert T0. The adhered material mainly consists of Fe elements. The adhesion on textured insert appears large area aggregation especially near the edge of texture, which is mainly due to the derivative cutting behavior of the micro-texture. The adhesion can cover the textures if it is serious. Then, the effect of micro-textures on tool-chip interface friction will be weakened. If the machining time is long enough, the textures will be all covered by adhesion, and the average friction coefficient of textured insert will be the same as untextured insert, as shown in Fig. 8. In addition, on the rake face of untextured insert, built-up edge (BUE) appears. Here, the BUE will replace the main cutting edge and participate in the machining process. Then, it will increase the actual working rake angle r_{oe} and reduce the cutting forces during the machining. Therefore, cutting force of untextured insert in Fig. 8 shows an obvious decreasing trend at the beginning. However, the micro-textures have shown a positive effect on the wear behavior. It can reduce the tool-chip interface frictional force, which can reduce the cutting temperature. Then, the BUE is suppressed during the machining with textured insert. The BUE structure is instable during the machining process. It will lead to a destruction of the workpiece surface and reduce the tool life. Thus, the micro-textures can

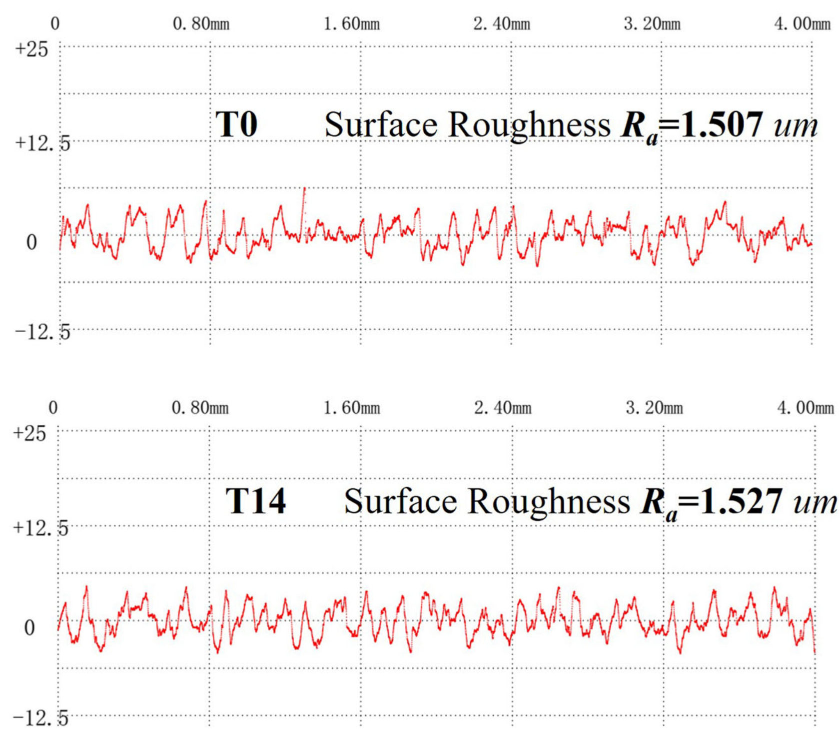

Fig. 9 Roughness of machined surface with untextured and textured inserts

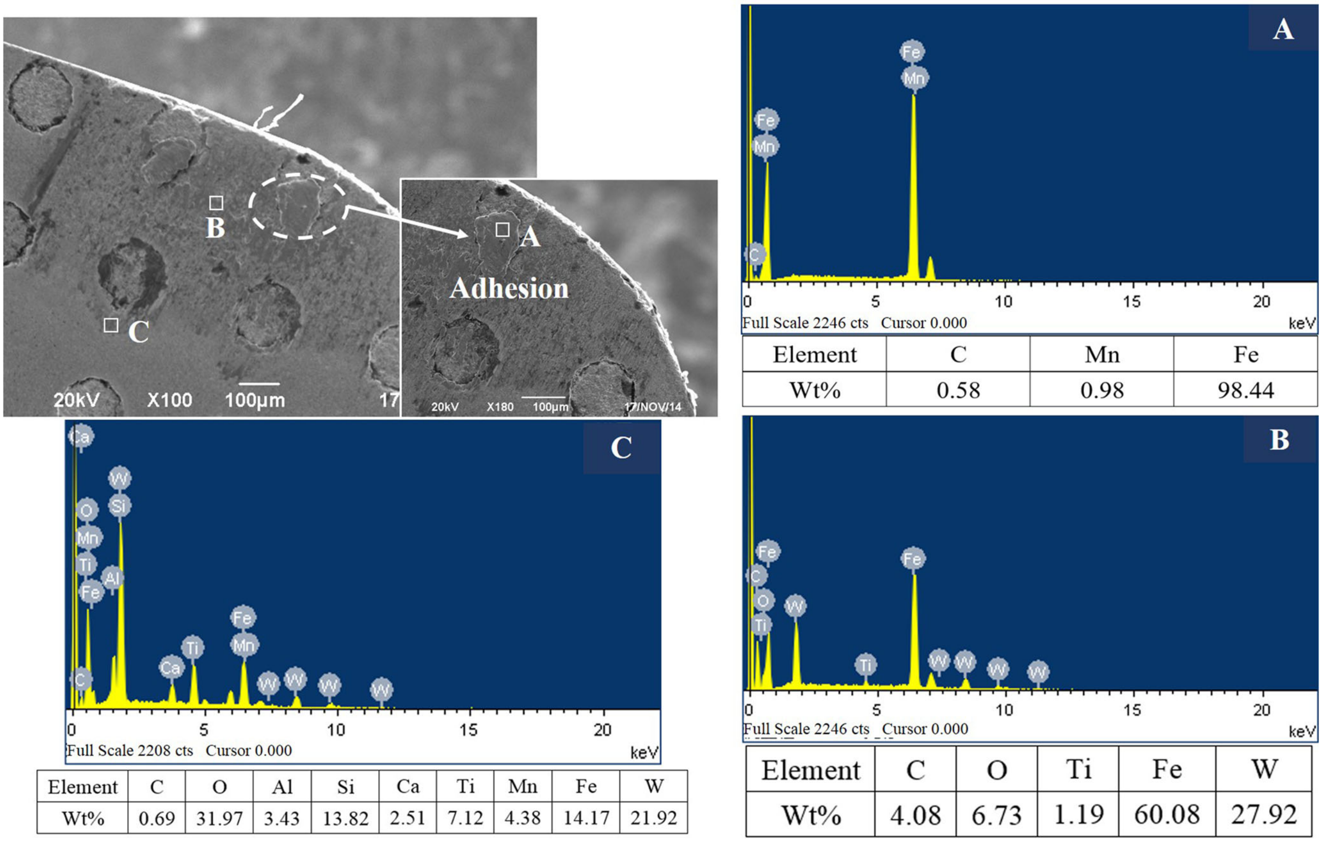

A

Element	C	Mn	Fe
Wt%	0.58	0.98	98.44

B

Element	C	O	Ti	Fe	W
Wt%	4.08	6.73	1.19	60.08	27.92

C

Element	C	O	Al	Si	Ca	Ti	Mn	Fe	W
Wt%	0.69	31.97	3.43	13.82	2.51	7.12	4.38	14.17	21.92

Fig. 10 SEM and EDS results of the rake face of textured insert T14

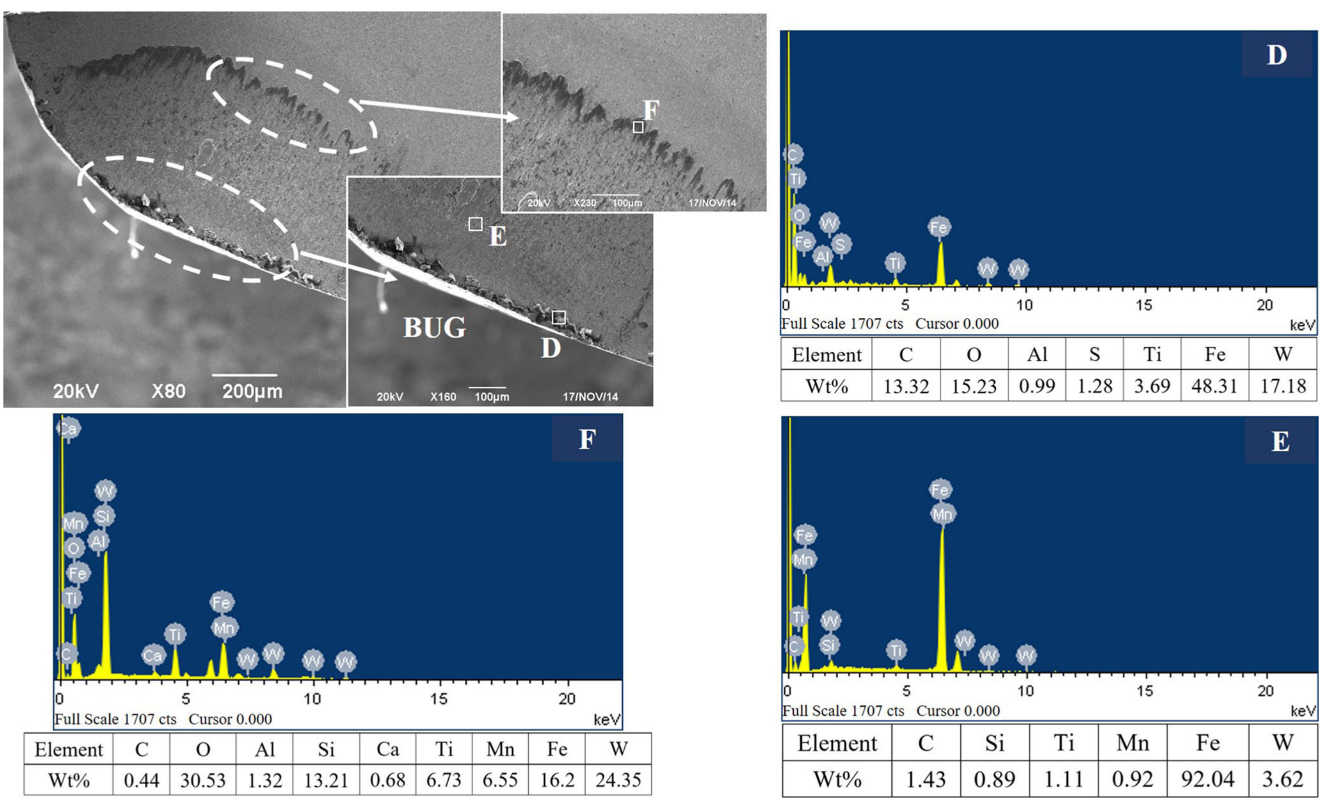

D

Element	C	O	Al	S	Ti	Fe	W
Wt%	13.32	15.23	0.99	1.28	3.69	48.31	17.18

E

Element	C	Si	Ti	Mn	Fe	W
Wt%	1.43	0.89	1.11	0.92	92.04	3.62

F

Element	C	O	Al	Si	Ca	Ti	Mn	Fe	W
Wt%	0.44	30.53	1.32	13.21	0.68	6.73	6.55	16.2	24.35

Fig. 11 SEM and EDS results of the rake face of untextured insert T0

effectively suppress the formation of BUE and improve the cutting performance.

Additionally, a lot of Fe and O elements appeared on the worn area of both textured insert and untextured insert. The Fe elements mainly come from the workpiece material, and O elements come from the air. It indicates that the diffusion wear and oxidation wear occur during the machining. Figures 10 and 11 show that the percentages of Fe elements on the rake face of T14 (region B) and T0 (region E) are about 60% and 90%, respectively. It will destroy the surface chemical composition and strength of insert rake face. The textured insert presents a lower Fe element diffusion. The cutting temperature is a key factor for diffusion wear. Here, the temperature rise is mainly caused by the shear heat of workpiece and tool-chip interface frictional heat. The micro-textures on the rake face can effectively reduce the average friction coefficient, average shear strength, and frictional force at the tool-chip interface. Therefore, the cutting temperature will be reduced with the decreasing of tool-chip interface frictional heat. Then, the diffusion wear will be suppressed in the textured insert with lubrication. Here, the O elements are observed at the edge of the worn area of T14 (region C) and T0 (region F). The normal stress is relatively small in this place for it is far from the main cutting edge. Then, the air enters the tool-chip interface during the machining. However, no O element is found on the worn area near the main cutting edge of T0 (region E). This is mainly due to the high normal stress in this area. It makes the air hardly enter the close contact interface. The situation is different when it comes to textured insert T14. Few O elements are found on the worn area near the main cutting edge (region B). The micro-textures can store a small amount of air while storing the cutting fluids. So that, even in the close contact area of the tool-chip interface, air participates in the reaction during the machining. Then, few O elements are observed in this area.

These results indicated that adhesive wear, diffusion wear, and oxidation wear appeared during the machining of AISI 1045 steel with lubrication. The introduction of micro-textures can effectively reduce the average shear strength and improve the wear behavior during the machining. Especially, the diffusion wear and BUE structure on the rake face are significantly reduced with textured insert. However, further works are still needed on the stability of BUE structure with different cutting parameters and derivative cutting behavior of the micro-texture.

4 Conclusions

In this work, the influence of micro-textures on the wear mechanism of WC-TiC/Co cemented carbide inserts was studied by experimental observations and theoretical analysis. The results showed that the introducing of micro-texture on the certain place can effectively reduce the cutting force, tool-chip interface friction coefficient, and improve the wear behavior.

The micro-pits on the rake face can reduce the average shear strength by increasing the contact area of lubricant. The tool-chip interface friction coefficient and frictional force will be much lower when compared with untextured insert. A suitable texture parameter can fully improve the lubrication performance while maintaining the insert strength. Here, a lower value of average friction coefficient was obtained with texture diameters: $d = 170$ μm, depth $h = 7$ μm, and area occupancy $w = 20\%$.

Derivative cutting behavior of the micro-textures will come up during the machining. It can form the aggregation of adhesion near the edge of texture. Then, the advantages of micro-textures will disappear if the machining time is long enough. The BUE structure will appear on the main cutting edge with untextured insert in this research. It can reduce the cutting force by increasing the actual working rake angle. However, the textured insert can effectively suppress the formation of BUE with a better wear behavior and a lower cutting temperature.

Adhesive wear, diffusion wear, and oxidation wear appeared during the machining of AISI 1045 steel with YT15 inserts under lubrication condition. The Fe elements in the workpiece material will spread to the rake face and destroy the surface strength of the insert during the machining. The textured insert can effectively suppress the diffusion of Fe elements by reducing the tool-chip interface frictional heat. Oxidation wear can even appear on the textured insert worn area near the main cutting edge. It is mainly due to the micro-textures can store part of air while storing the cutting fluids.

Acknowledgments This work was mainly supported by the Fundamental Research Funds for the Central Universities [grant number JZ2020HGTA0084 and JZ2019HGBZ0118]. The authors also thank Institute of Tribology, Hefei University of Technology, for their contributions to the texture manufacturing.

References

1. Sharma V, Pandey PM (2016) Recent advances in turning with textured cutting tools: a review. J Clean Prod 137:701–715
2. Orra K, Choudhury SK (2018) Tribological aspects of various geometrically shaped micro-textures on cutting insert to improve tool life in hard turning process. J Manuf Process 31:502–513
3. Arslan A, Masjuki HH, Kalam MA, Varman M, Mufti RA, Mosarof MH, Khuong LS, Quazi MM (2016) Surface texture manufacturing techniques and tribological effect of surface texturing on cutting tool performance: a review. Crit Rev Solid State 41(6):447–481
4. Ghosh P, Pacella M (2020) Effect of laser texturing on the performance of ultra-hard single-point cutting tools. Int J Adv Manuf Technol 106:2635–2648

5. Qian XH, Duan XY, Zou JY (2020) Effects of different tool microstructures on the precision turning of titanium alloy TC21. Int J Adv Manuf Technol 106:5519–5526
6. Ge D, Deng J, Duan R, Liu Y, Li X, Yue H (2019) Effect of micro-textures on cutting fluid lubrication of cemented carbide tools. Int J Adv Manuf Technol 103:3887–3899
7. Liu X, Liu Y, Li L, Tian Y (2019) Performances of micro-textured WC-10Ni_3Al cemented carbides cutting tool in turning of Ti6Al4V. Int J Refract Met H 84:104987
8. Duan R, Deng J, Lei S, Ge D, Liu Y, Li X (2019) Effect of derivative cutting on machining performance of micro textured tools. J Manuf Process 45:544–556
9. Duan R, Deng J, Ai X, Liu Y, Chen H (2017) Experimental assessment of derivative cutting of micro-textured tools in dry cutting of medium carbon steels. Int J Adv Manuf Technol 92:3531–3540
10. Wei Y, Kim MR, Lee DW, Park C, Park SS (2017) Effects of micro textured sapphire tool regarding cutting forces in turning operations. Int J Pr Eng Man-gt 4(2):141–147
11. Kümmel J, Braun D, Gibmeier J, Johannes S, Greiner C, Schulze V, Wanner A (2015) Study on micro texturing of uncoated cemented carbide cutting tools for wear improvement and built-up edge stabilisation. J Mater Process Technol 215:62–70
12. Li W, Zhang Z (2019) Effect of cutting tool with micro-pits texture on wood cutting performance. PLoS One 14(4):e0214888
13. Liu X, Liu Y, Li L, Tian Y (2019) Optimization of the micro-textures on the cutting tool based on the penetration of the lubricant in the micro-textures. Int J Adv Manuf Technol 104:3173–3180
14. Ye D, Lijun Y, Bai C, Xiaoli W, Yang W, Hui X (2018) Investigations on femtosecond laser-modified microgroove-textured cemented carbide YT15 turning tool with promotion in cutting performance. Int J Adv Manuf Technol 96:4367–4379
15. Sun J, Zhou Y, Deng J, Zhao J (2016) Effect of hybrid texture combining micro-pits and micro-grooves on cutting performance of WC/co-based tools. Int J Adv Manuf Technol 86:3383–3394
16. Alagan NT, Zeman P, Hoier P, Beno T, Klement U (2019) Investigation of micro-textured cutting tools used for face turning of alloy 718 with high-pressure cooling. J Manuf Process 37:606–616
17. Durairaj S, Guo J, Aramcharoen A, Castagne S (2018) An experimental study into the effect of micro-textures on the performance of cutting tool. Int J Adv Manuf Technol 98:1011–1030
18. Pang M, Liu X, Liu K (2019) Effect of conical micro-grooved texture on tool-chip friction property and cutting performance of WC-TiC/co cemented carbide tools. P I Mech Eng J-J Eng 233(5):791–804
19. Pang M, Nie Y, Ma L (2018) Effect of symmetrical conical micro-grooved texture on tool-chip friction property of WC-TiC/co cemented carbide tools. Int J Adv Manuf Technol 99:737–746
20. Gürgen S, Çakır F, Sofuoğlu M, Orak S, Kuşhan M, Li H (2019) Multi-criteria decision-making analysis of different non-traditional machining operations of Ti6Al4V. Soft Comput 23:5259–5272
21. Gajrani KK, Suresh S, Sankar MR (2018) Environmental friendly hard machining performance of uncoated and MoS_2 coated mechanical micro-textured tungsten carbide cutting tools. Tribol Int 125:141–155
22. Gajrani KK, Reddy RPK, Sankar MR (2019) Tribo-mechanical and surface morphological comparison of untextured, mechanical micro-textured (MuT), and coated-MuT cutting tools during machining. P I Mech Eng J-J Eng 233(1):95–111
23. Xing Y, Deng J, Wu Z, Liu L, Huang P, Jiao A (2018) Analysis of tool-chip interface characteristics of self-lubricating tools with nanotextures and WS_2/Zr coatings in dry cutting. Int J Adv Manuf Technol 97:1637–1647
24. Sharma V, Pandey PM (2016) Comparative study of turning of 4340 hardened steel with hybrid textured self-lubricating cutting inserts. Mater Manuf Process 31:1904–1916
25. Feng Y, Zhang J, Wang L, Zhang W, Tian Y, Kong X (2017) Fabrication techniques and cutting performance of micro-textured self-lubricating ceramic cutting tools by in-situ forming of Al_2O_3-TiC. Int J Refract Met H 68:121–129
26. Kang Z, Fu Y, Chen Y, Ji J, Fu H, Wang S, Li R (2018) Experimental investigation of concave and convex micro-textures for improving anti-adhesion property of cutting tool in dry finish cutting. Int J Pr Eng Man-gt 5(5):583–591
27. Song WL, Wang ZC, Wang SJ, Zhou K, Guo ZX (2017) Experimental study on the cutting temperature of textured carbide tool embedded with graphite. Int J Adv Manuf Technol 93:3419–3427
28. Arulkirubakaran D, Senthilkumar V, Dinesh S (2017) Effect of textures on machining of Ti-6Al-4V alloy for coated and uncoated tools: a numerical comparison. Int J Adv Manuf Technol 93:347–360
29. Sugihara T, Enomoto T (2017) Performance of cutting tools with dimple textured surfaces: a comparative study of different texture patterns. Precis Eng 49:52–60
30. Ozlu E, Budak E, Molinari A (2009) Analytical and experimental investigation of rake contact and friction behavior in metal cutting. Int J Mach Tool Manu 49:865–875
31. Budak E, Ozlu E (2008) Development of a thermomechanical cutting process model for machining process simulations. CIRP Ann Manuf Technol 57:97–100
32. Song W, Deng J, Zhang H, Yan P (2010) Study on cutting forces and experiment of MoS_2/Zr-coated cemented carbide tool. Int J Adv Manuf Technol 49(9–12):903–909